Cost Modeling and Depreciation for Reused Powder Feedstocks in Powder Bed Fusion Additive Manufacturing

Michael Barclift[1], Sanjay Joshi[2], Timothy Simpson[1,2,3], and Corey Dickman[3]

[1]Department of Mechanical and Nuclear Engineering
[2]Department of Industrial and Manufacturing Engineering
[3]Center for Innovative Materials Processing through Direct Digital Deposition (CIMP-3D)
The Pennsylvania State University, University Park, PA 16802

Abstract

Cost modeling for Powder Fusion (PBF) has traditionally treated the material feedstock as a fixed cost. Given that a built-up geometry in PBF must be in a bed filled with surrounding powder, the material feedstock is susceptible to satellites, chemical contamination, and dissimilar properties with each subsequent reuse. In this paper, we extend an existing PBF cost model and propose a new financial depreciation model for reused metal powders. Using Sum-of-the-Years Digits depreciation, powder feedstock is valued as a function of build cycles endured by the material feedstock. A case study is presented on two example parts in Direct Metal Laser Sintering (DMLS). Results show that cost models using a fixed material cost can undervalue build jobs with a high value virgin powder by as much as 3-11% or 13-75% depending on the material and its maximum build cycles in PBF.

Introduction

Additive Manufacturing (AM) is a process of "joining materials to make objects from 3D model data, usually layer upon layer" [1]. Powder Bed Fusion (PBF) is one AM process where "thermal energy selectively fuses regions of a powder bed" to produce parts [1]. As shown in Figure 1, PBF consists of a powder delivery system, where a feed bed (i.e., hopper, dispenser) supplies a layer of powder onto a part bed containing the build job geometries. Thermal energy from an electron-beam or laser scans the part bed surface and fully melts a region of powder particles to form a solidified cross-section. The powder bed lowers and a coating mechanism, (i.e., blade, rake, roller) spreads additional powder from the feed bed on top of the scanned layer. Energy is applied to the newly recoated surface, and the AM process repeats for each layer until all geometries have been fabricated. At the completion of the build job, parts are removed from the machine, while surrounding un-melted powder is recovered from the part bed and overflow bin for reuse in later builds. PBF is commonly executed in a build chamber filled with inert gas (e.g., Argon, Nitrogen) or under vacuum to mitigate the reactivity of the powder feedstock during the melting of each cross-section.

Technologies for PBF include Direct Metal Laser Sintering (DMLS), Selective Laser Melting (SLM), Direct Metal Laser Melting (DMLM), Direct Metal Printing (DMP), Laser Melting (LM), LaserCUSING, and Electron Beam Melting (EBM) [3]. In comparison to polymeric AM processes, PBF with metal powder feedstocks requires extensive labor in order to generate a fully-functional component. In laser-powered PBF, digital modeling of the part orientation and support structures is a non-trivial task, with the goal of anchoring [4] the part to the build substrate. This design process is important due to the risk of thermal distortion and delamination during the build [5]. In electron-beam PBF, the heated powder bed can mitigate

thermal distortion; however, the design of the support structures may need to be conducted in a manner to dissipate heat or minimize curling for fine features [6]. Finally, after a completed build job, PBF parts can have internal voids (i.e., porosity) and residual stress, which requires post-processing via stress relief, heat treatment, annealing, shot peening, hot isostatic pressing (HIP), or tomographic inspection in order to meet performance requirements [7].
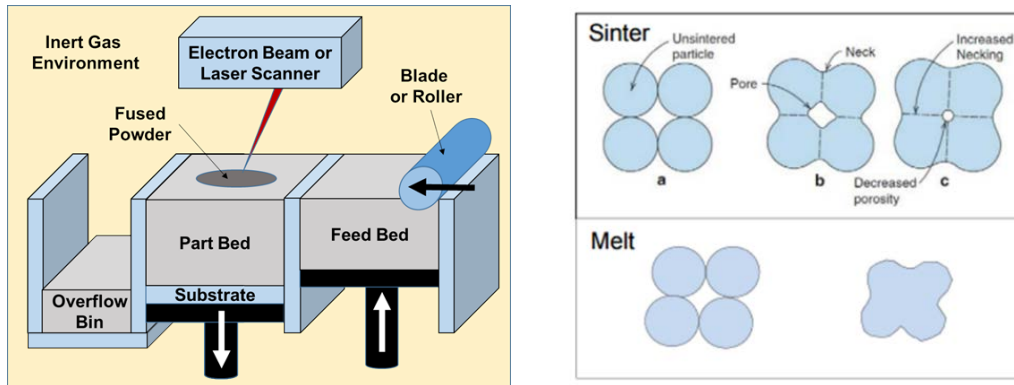

Figure 1. Powder Bed Fusion Schematic (left) and Fusing of Powder Particles (right) [2]

With differences pertaining to their energy source, control mechanisms, and operating conditions [8], PBF technologies share a common feedstock in metal powder, a material which can range in price from "$260 to $450 per kg" [9]. Due to this expense, un-melted feedstock is reused, also referred to as recycled, in subsequent build jobs to save costs over purchasing additional virgin powder [10]. Despite these savings, reused powder endures partial sintering with each AM build due to latent heat from the melt-pool, leading to subsequent changes in the powder size distribution [11]. This phenomenon creates non-spherical particles and satellites leading to porosity and rough surfaces [12]. In parallel, the formation of oxides, soot, and exposure to ambient atmosphere can disseminate chemical impurities in the feedstock [7, 13]. With many of these AM technologies having "black box" controllers [14], users are restricted to proprietary materials and process parameters provided by the Original Equipment Manufacturer (OEM), limiting options for customized processing conditions or alternative feedstock suppliers.

The objective in this paper is to answer the following research question: "*How does the reusability of a metal powder feedstock impact the total costs in PBF?*" To answer this question, we extend an existing PBF cost model and present a case study detailing the costs for two parts built in a PBF process. Beginning with a literature review in Section 2, previous work on AM cost modeling is summarized along with current research on powder reusability in AM. Section 3 discusses the expanded cost model along with the proposed formulas and variables. Section 4 provides an overview of the case study, followed by results and closing remarks in Section 5 and 6, respectively.

2. Literature Review

2.1. Cost Modeling in Additive Manufacturing

Lindemann et al. [15] performed a lifecycle study for production in metal additive manufacturing (AM) using Time-driven Activity-Based Costing (ABC). Costs for a generic

metal AM machine were discretized into an activity workflow of CAD Preparation, Machine Preparation, Build Process, Support Removal, and Surface Treatment. Considering a single part geometry for production at 4500 h/year, their cost model found that 74% of total costs can be attributed to machine costs, followed by material costs at 12%. Sensitivity analysis revealed that the material costs could vary between 5% and 46% of the total cost based on the value of the material feedstock.

Rickenbacher et al. [16] expanded the work of Lindemann et al. by proposing a generic cost model for SLM. Rickenbacher et al. used ABC while accounting for multiple geometries and additional part quantities in the same AM build. Costs associated with the build time for a multiple geometry build job were evenly divided among all the parts in a layer-wise manner, based on their respective build heights. In a case-study for three geometries, Rickenbacher et al. found that a cost savings of 41% can be achieved by building up the parts together in the same build job instead of individual builds, agreeing with observations found by Lindemann et al. The total build time was identified as the largest cost driver in the workflow due to machine costs associated with exposing each layer of powder. One limitation for both of these models is that they treated the material feedstock as a fixed cost and did not allocate a cost for changes in the powder's properties and overall value as the material was being processed and reused in PBF.

2.2. Metal Feedstocks in Powder Bed Fusion

Metal powder is defined as a substance containing particles of elemental metals or alloys, normally less than 1000 microns in size [17]. This substance can be produced through various electro-chemical and thermo-mechanical processes such as Gas Atomization, Water Atomization, Centrifugal Disintegration [18-20]. In metallurgical applications, the powder can be characterized by the Density, Powder Size Distribution (PSD), Chemical Composition, Surface Chemistry, Morphology, Crystalline Phases, Flowability, and Thermal Properties [13, 14]. Variability in powder properties can occur at numerous stages throughout the lifecycle of the material. Axelsson [21] conducted a study on Ti-6Al-4V powder produced from three independent manufacturers for EBM. Analysis of the chemical compositions found Nitrogen, Chlorine, and Yttrium outside ASTM F2924 limits, indicating contamination during the feedstock production process. Powder is also sensitive to oxidation, a naturally occurring chemical reaction where oxygen atoms undergo diffusion and exchange electrons with a metallic element to form oxides [22]. Oxides form surface films which can alter the absorptivity and melting of the material [23]. In addition to oxidation, the build environment of PBF machines can promote the formation of carbides and nitrides due to prolonged durations and reactivity at elevated temperatures [24].

Reusability refers to the ability of a powder to be reused in an AM process before it no longer conforms to standard specifications or fails to produce acceptable quality as defined by the "component supplier or purchaser" [25-28]. While reused powder can be physically sieved by particle diameter, the presence of chemical impurities, non-spherical agglomerates, and oxides may not be explicitly removed from the powder lot. In one study, Seyda et al. [29] took virgin Ti-6Al-4V powder and reused it in 12 DMLS build cycles to study changes in mechanical properties. Reusing the powder caused the PSD to increase and particles to become coarse due to the formation of partially-sintered agglomerates, shown in Figure 2. This correlated to surface roughness increasing from 92 to 123 Ra after the 12 build cycles. With no post-processing, test

specimens showed the ultimate tensile strength (UTS) increased from 1030 MPa to 1101 MPa after 6 build cycles, before decreasing to 1072 MPa for the last 6 reuses. The total amount of porosity in the produced parts decreased from 0.11% to 0.05%; however, the size of individual pores increased due to the enlarged PSD. Seyda et al. identified these pores as the cause for stress concentrations and localized defects.
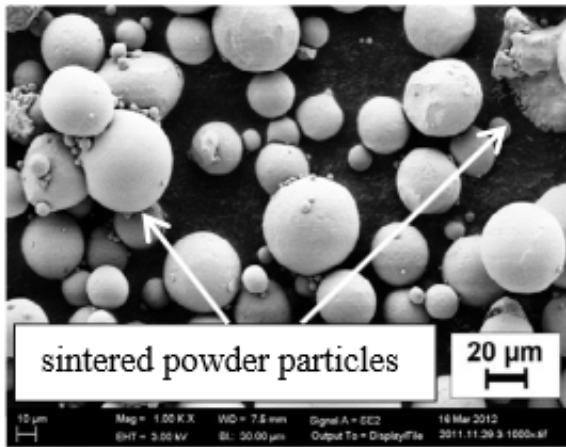

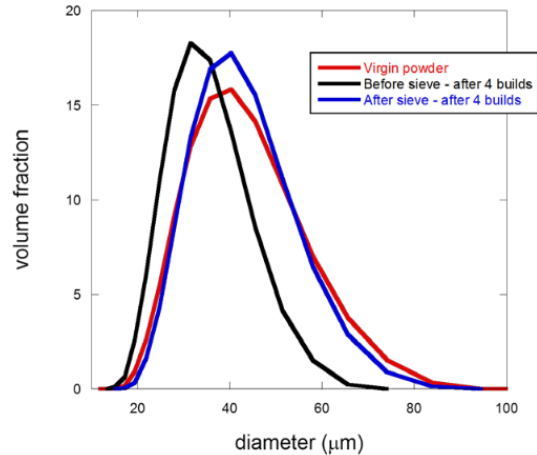Figure 2: Agglomerates in Reused Ti-6Al-4V[29]

Figure 3: PSD of 17-4SS [13]

Slotwinski et al. [13] studied stainless steel (17-4 SS) and cobalt chrome (CoCr) virgin powder, and reused them for eight DMLS build cycles to analyze changes in physical and chemical properties. Reusing the powder caused the volume fraction to increase with reuses as shown in Figure 3. Agglomerates formed in the AM process continually passed through the sieve due to their morphology or they were scrapped away by the recoating mechanism in the AM process. Overall, these particles could not be explicitly removed from the powder. The 17-4 SS and CoCor powder feedstocks were analyzed by x-ray photospectroscopy (XPS) and showed no significant difference in the elemental composition of the sieved powder after 8 build reuses. However, a comparison of the sieved 17-4SS powder and sieve residue revealed significant differences in the surface chemistry and crystalline phases.

Tang et al. [30] reused Ti-6Al-4V ELI virgin powder for 21 build cycles in EBM, sieving the powder at 177 microns. Oxygen content increased with each reuse from 0.08 wt.% to 0.19 wt.%, as presented in Figure 4. The oxygen content directly correlated to the UTS but not the elongation. UTS increased from 920 MPa to 1039 MPa, while elongation was scattered between 13-18%. Tang et al. identified that oxygen may be reacting with the powder as parts are being removed from the build chamber, sieving, or as parts are being cleaned in the Arcam Powder Recovery System. In conjunction, oxygen pick-up was attributed to exposure time in the build job along with ambient humidity in the laboratory. Since the powder progressively gained oxygen, Tang et al. suggest that Ti-6Al-4V ELI should not be reused more than 4 times in EBM to maintain compliance with ASTM F3001 (Grade 23). Alternatively, another recommendation was to replenish the reused powder lot with additional virgin powder to stabilize the oxygen content and stay "in-spec" with the provided standard.

Grainger [31] conducted a similar study LM wherein Ti-6Al-4V ELI powder lot was used in 38 build cycles, with no additional virgin powder. The results shown in Figure 5 illustrated a

similar trend of increasing oxygen content with each build job, and exceeding the specification for ASTM F3001 between 15-35 build cycles, yet still within acceptable limits for Grade 5 titanium. With no significant variation observed in the tensile properties and chemical pickup, Grainger concluded that there was no requirement to dispose of un-melted Ti-6Al-4V powder after it had been cycled through a number of reuses. However, Grainger noted that the results could not be extended to other AM machines and materials due to differences in how a PBF technology generates the inert atmosphere and their mechanisms for powder handling.
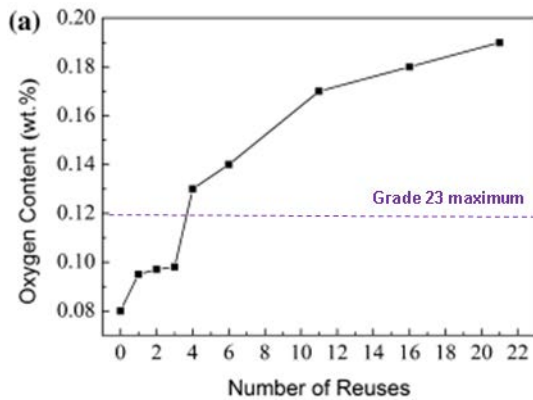

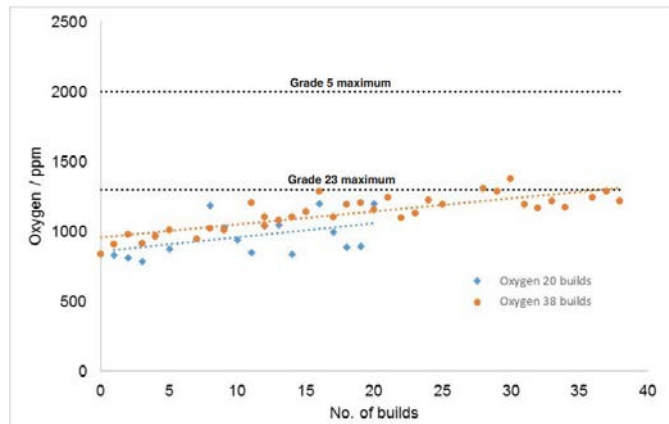Figure 4: Oxygen buildup in Ti-6Al-4V ELI during EBM [30]

Figure 5: Oxygen buildup in Ti-6Al-4V ELI during LM [31]

2.3. Summary of Literature Review and Current Gaps

With material costs ranging between 5-46% [15] of the total costs in metallic PBF processes, current cost models are assuming a constant, fixed cost, for the material feedstock and financially valuing reused powder as virgin powder. These models lack an analytical method for determining the value of the reused material as it undergoes physical and chemical changes in subsequent build jobs. The reusability of powder feedstock can vary across material alloys and PBF technologies due to the production process of the powder, energy-material interaction for a given machine, powder sieving/handling, and build chamber environments. While reactive metals such as 17-4 SS and Ti-6Al-4V ELI may attain chemical impurities with subsequent build jobs, other alloys such as IN718 may have virtually identical material composition when replenishing the lot with virgin powder [32]. While some studies have found little to no variation in the tensile properties, present literature is limited on the impact of reused powder on fatigue properties and correlating them to mixing virgin/reused feedstocks along with process parameters (e.g., power, scan velocity, hatch spacing, tool path) [23].

3. Powder Costing Methodology

3.1. Financial Depreciation for Costing Powder Feedstocks

As discussed in the previous section, the reusability of a powder feedstock is not explicitly captured in current AM cost models due to the use of a fixed material cost. This creates uncertainty as to how one should financially value the feedstock as it is reused in PBF and how to precisely cost parts produced from a reused feedstock. To correlate reusability to the

price of a powder feedstock, we propose that the material used in PBF be valued through a financial depreciation model. In accounting practice, depreciation is defined as the "gradual decline in the financial value of property due to increasing age and eventual obsolescence" [33]. With the risk of oxides, porosity, surface roughness, and chemical contamination, the quality of the powder feedstock diminishes as it is continually reused in PBF. Using a depreciation model, we can model the systematic loss in a feedstock's value proportional to the powder's degraded properties over a given duration of time.

Although depreciation is traditionally used in business accounting for the United States' Internal Revenue System [34], we are proposing depreciation strictly in the context of a costing method for PBF. Depreciation is a function of the maximum allowable time duration for the feedstock and its salvage value, estimated market value, when it has reached the end of its useful life. Due to AM parts having individually-tailored functions and design applications, current material standards have resorted to agreement between component supplier and the purchaser for determining the acceptance of a reused powder in AM [25-28]. As discussed previously in Section 2.3, with each powder feedstock having a unique elemental composition and PBF technology, its corresponding time duration for reusability will vary based on factors related to the build chamber environment, energy-material interaction, and powder handling.

Three common depreciation models are: Straight-Line (SLN), Double Declining Balance (DDB), and Sum-of-the-Year's Digits (SOYD) [35] as shown in Figure 6. SLN assumes a uniform reduction in value with each increment in time; however, this linear depreciation is fixed and assumes that the powder feedstock loses uniform amounts of value regardless of being at the beginning or end of its useful life. With virgin powder being at most risk of chemical contamination and oxides, an ideal depreciation model is one that reflects a relatively large rate of decline after initial uses in a PBF process and then a smaller rate as the feedstock is continually reused to correspond to compounded degradation over time. DDB presents a more accelerated model where the feedstock rapidly loses value at early stages of its useful life and then gradually less in later life; however, since DDB applies a constant multiplier for depreciation, the salvage value is not explicitly designated and therefore unadaptable to whichever value the user designates for the end-use scrap, unless manually corrected. Serving as a median between SLN and DDB, SOYD exhibits a moderate drop in value at early life and less as the material is increasingly reused. A possible drawback for SOYD is that it does not depreciate as rapidly as the DDB. Unlike DDB, the salvage value of SOYD can be specified by the user making it a more flexible and adaptable model for a wide range of materials. Given these customizable features and appropriate depreciation rates, SOYD was selected as the most suitable model for valuing a powder feedstock as it is reused in PBF.

With SOYD as the selected depreciation model, units needed to be specified for the time duration in which the powder feedstock is reused. Build cycles are widely cited in the research [29-32]; however, build cycles are an imprecise measure due to variations in the underlying build time, build height, part orientation, and quantity of parts. While an AM build job is typically measured in units of hours [2], this value can be convoluted with the idle time and recoating time of the AM machine. While time durations can measure temporal usage, it does not provide insight on the explicit process parameters and build chamber conditions in which a powder feedstock was processed.
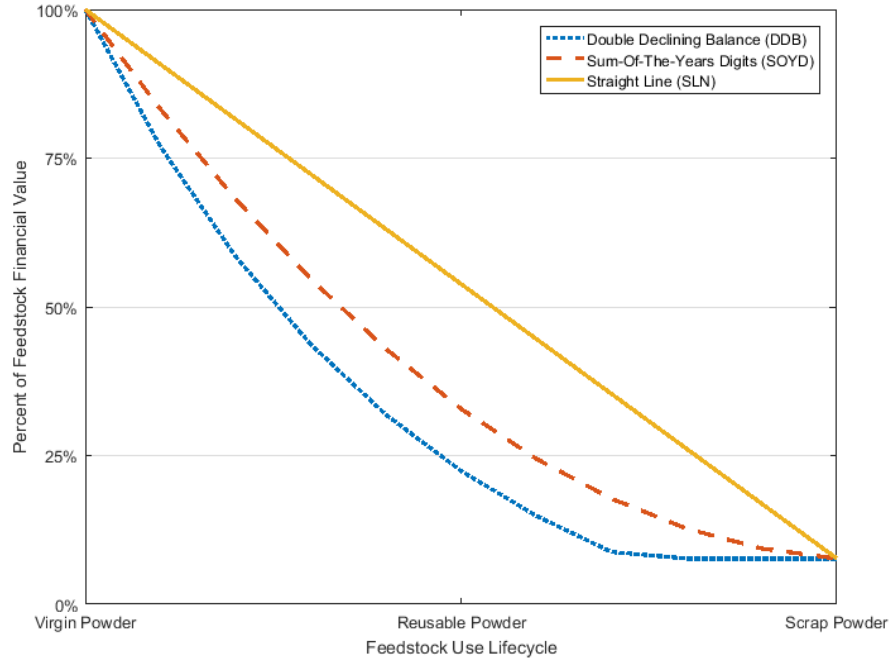
Figure 6: Comparison of Depreciation Methods for Powder Feedstock

Given the present information in literature and limited alternatives, build cycles was selected as the unit for measuring the time duration of a powder feedstock in PBF. Equation 1 is our proposed method for valuing the powder feedstock using SOYD. For this equation, it is assumed that a powder lot is reused on a single AM machine, where the overflow, part bed, and feed bed powder are mixed and sieved after each build. Builds are conducted using consistent process parameters, atmosphere, material handling conditions, and have no added virgin powder.

$$C_{m_{u+1}} = Cm_u - (Cm_0 - S) \cdot \left(\frac{U_{max} - u + 1}{\frac{U_{max}(U_{max} + 1)}{2}} \right) \tag{1}$$

where:
Cm_u is the cost of the powder feedstock that has been used u times ($/kg),
Cm_0 is the cost of a virgin powder feedstock ($/kg),
S is the salvage value of the powder at the end of its depreciable life ($/kg),
U_{max} is the maximum number of build cycles a powder can be used for a PBF technology (-),
u is the number of build cycles a powder has underwent in PBF (-).

3.2. Activity-Based Cost Modeling for Powder Bed Fusion

To implement the proposed model for valuing a reused powder, we expand upon the work of Rickenbacher et al. [16] and follow a similar workflow to that shown in Figure 7. A built-up AM part, P_i, shall consist of geometry, G_i with N_i quantity in a build job for PBF. Due to overlap with the previous model by Rickenbacher et al., we only present equations that have been modified or are unique to this paper.
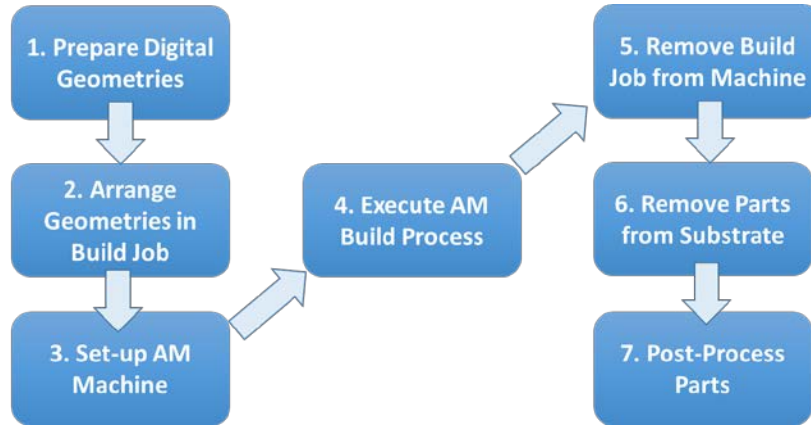
Figure 7: Rickenbacher et al.'s Workflow for SLM [16]

The first labor activity in this cost model is the preparation of the digital geometry data [16]. Upon receiving the costumer's digital model, it is assumed that the geometry meets general Design for AM rules (e.g., process selection, fully enclosed surfaces, wall thickness, tolerances) [36-38]. The tasks in this activity are selecting a build orientation and generating support structures. Software packages such as NetFabb and Materialise Magics [39, 40] can automate these processes; however, these programs are not robust for metal AM and may produce designs that satisfy manufacturing requirements but fail to meet product specifications [41]. Thus, this activity is an iterative process that relies on experiential knowledge of the AM operator and must be tailored to the given PBF technology and geometry.

Once all of the parts have been successfully prepared for AM, the digital geometries are read into a build layout program. The manipulation and placement of geometries on the digital build tray can have repercussions regarding the likelihood of build failure (e.g., collision with recoating mechanism, curling, surface roughness) [6, 42]. With limited literature and standards for this activity, it is also conducted in an iterative manner relying on previous knowledge and past experience. The time required for arranging the geometries is a function of the total part geometries and replicates present in the AM build job.

Machine set-up consists of uploading the digital build tray files, selecting process parameters, initializing inert gas (or vacuum depending on PBF technology), and readying system hardware. With metal powders having explosive and physiological hazards [2, 7, 43-45], material handling is dangerous, requiring timely and duteous tasks for safe activity. Additional time can occur if the build calls for a different material than the one currently loaded in the machine. The total time for changing materials includes the tasks of unloading the current powder, cleaning the build chamber, replacing consumables (e.g., filters, inert gas), loading the new feedstock, and cleaning all ancillary equipment (i.e., vacuum). While Rickenbacher et al. use empirical factors for extra effort under inert environment and material change frequency, they have been removed since they are captured in the machine set-up and material change time, as shown in Equation 2.

$$C_{setup}(P_i) = (C_{op} + C_{Mach}) \cdot \frac{(T_{setup} + T_{mat.change})}{\sum_i N_i} \qquad (2)$$

where:
C_{setup} is the cost per part for setting up the AM machine ($),
P_i is the built-up AM part corresponding to ith geometry (-),
C_{Mach} is the AM machine's hourly rate ($/h),
C_{oper} is the operator's hourly rate ($/hour),
T_{setup} is the time for setting up the machine (h),
$T_{mat.change}$ is the total time for changing the material, including corresponding activities (h),
N_i is the quantity of parts with ith geometry (-).

The derivation of a high-fidelity build-time estimator is outside the scope of this paper. With commercial solutions available through software and the AM machine's preprocessors [46], we instead defer to a generic formula for calculating individual build times in lieu of the previous regression model specific to SLM [2, 47]. For build jobs with multiple parts, this formula assumes that the build rate for exposing each voxel is constant and that all time latency due to positioning the energy scanner between consolidated powder regions is negligible. Using the algorithm proposed by Rickenbacher et al. [16], the recoating time for build jobs with multiple build heights is calculated in a time fraction manner for each part:

$$T_{build}(P_i) = \frac{T_{idle}}{\sum_i N_i} + T_{build\ speed} \cdot \sum_i (N_i \cdot V_{total_i}) + T_{recoat}(P_i) \tag{3}$$

where:
T_{build} is the total time required for building up a single part in a given build job (h),
P_i is the built-up AM part corresponding to ith geometry (-),
T_{idle} is the time when the AM machine is inactive (e.g., heating, cooling) (h),
$T_{build\ speed}$ is the average time for the AM machine to consolidate a voxel of powder (h/cm^3),
N_i is the quantity of parts with ith geometry (-),
V_{total_i} is the total volume of the part and support structures for ith geometry (cm^3),
T_{recoat} is the total recoating time allocated to a single part (h).

Once the operator has completed all hardware and software set-up, then the build job commences, and the AM machine proceeds to fabricate the designated part(s). To cost the activity of the AM machine throughout this duration, costs are grouped into three categories as shown in Equation 4. Machine costs includes costs pertaining to AM machine utilization and inert gas, multiplied by the build time allocated to a given part (see Equation 5). Material cost, as presented in Equation 6, is the cost related to the mass of the powder feedstock melted by the AM machine to produce the part. Using the concepts introduced in Section 3.1, the material costs is valued as a function of the build cycles endured by the material feedstock loaded in the AM machine. For the mass of the part, in Equation 7, empirical factors are included to compensate for powder losses due to particles trapped in the filters [48] during processing and loose powder trapped in hollow support structures.

$$C_{build}(P_i) = C_{build-Machine}(P_i) + C_{build-Material}(P_i) + C_{build-Depreciation}(P_i) \tag{4}$$

where:
C_{build} is the cost per part for building up a part using the AM machine ($),

P_i is the built-up AM part corresponding to ith geometry (-),
$C_{build-machine}$ is the cost per part for operating the AM machine during a build job ($),
$C_{build-material}$ is the cost per part for the melted powder feedstock in the AM process ($),
$C_{build-Depreciation}$ is the cost per part for the un-melted feedstock used in the AM process ($).

$$C_{build-machine}(P_i) = T_{build} \cdot (C_{mach} + C_{gas}) \tag{5}$$

where:
$C_{machine}$ is the cost per part for producing a build job in the AM process ($),
P_i is the built-up AM part corresponding to ith geometry (-),
T_{build} is the time for building up the entire job in the AM process (h),
C_{mach} is the AM machine's hourly operating cost ($/h),
C_{gas} is the cost for inert gas consumption during the build ($/h),
N_i is the quantity of parts with ith geometry (-).

$$C_{build-material}(P_i) = M_i \cdot Cm_u \tag{6}$$

where:
$C_{build-material}$ is the cost per part for the powder feedstock melted in the AM process ($),
P_i is the built-up AM part corresponding to ith geometry (-),
M_i is the mass of a part with ith geometry (kg),
Cm_u is the cost of the powder feedstock that has been used in u build cycles ($/kg).

$$M_i = (1 + \alpha) \cdot \rho_w \cdot (V_{part_i} + V_{supports_i}) + \gamma \cdot \rho_t \cdot V_{supports_i} \tag{7}$$

where:
M_i is the mass of a part with ith geometry (kg),
α is the percentage of powder loss due to process inefficiency (%),
γ is the percentage of powder loss due to being trapped within support structures (%),
V_{part_i} is the volume of the part body for the ith geometry (cm^3),
$V_{supports_i}$ is the volume of the support structures for the ith geometry (cm^3),
ρ_w is the powder wrought density (kg/cm^3),
ρ_t is the powder tap density (kg/cm^3).

In the third cost category, a build job requires powder feedstock to fill the powder bed and support built-up geometries throughout processing. This un-melted powder can become degraded by soot, oxides, and agglomerates during the AM process. These byproducts diminish the financial value of the feedstock, regardless of subsequent sieving, because the un-melted powder becomes populated with impurities that can propagate into future layers or builds. Thus, the un-melted powder loses the opportunity to be implemented as a virgin powder and produce parts with minimal defects from the base material. To allocate cost for this phenomenon, we propose that the financial value lost by the surrounding un-melted powder be charged to all parts produced within the build job. For this third category, the proposed cost is defined as Depreciation and calculated using Equation 8:

$$C_{build-Depreciation}(P_i) = \frac{M_i}{\sum_i(N_i \cdot M_i)} \cdot \left(M_{FB} - \sum_i (N_i \cdot M_i)\right) \cdot (Cm_u - Cm_{u+1}) \qquad (8)$$

where:
$C_{build-Depreciation}$ is the cost per part for the un-melted feedstock used in the AM process ($),
P_i is the built-up AM part corresponding to ith geometry (-),
M_i is the mass of a part with ith geometry (kg),
N_i is the quantity of parts with ith geometry (-),
M_{FB} is the total mass of the powder loaded into the AM machine's feed bed (kg),
Cm_u is the cost of the powder feedstock that has been used in u build cycles ($/kg).

In Equation 8, Depreciation cost is calculated by taking the mass of the powder loaded in the feed bed and subtracting the total mass of all built-up parts, including their corresponding powder losses. This is multiplied by the difference in financial value of the feedstock at its present state to the diminished value after one additional build cycle. Parts within the build job are allocated the Depreciation cost as a function of their mass fractions relative to the total mass of all built-up parts. Through Depreciation, this costing method accounts for the melting and, in-parallel, the degradation of the un-melted powder feedstock when building up a part in PBF. The calculation of the powder mass loaded in the feed bed is non-trivial and must be sufficient to fill the part bed completely and build-up the geometries. The amount of loaded powder feedstock is influenced by the material type and how a PBF technology accounts for changes in the levelling [7] of a layer as consolidated powder regions melt and re-solidify.

Once the AM process has finished building, the build job and all subsequent parts are physically removed from the AM machine. Equation 9 [16] takes the time required for this task and evenly divides it among the total number of parts created in the build job. Activities at this stage pertain to removing the build substrate from the machine, collecting all loose un-melted powder from the part bed, cleaning the machine, removing all powder from the feed bed and overflow bins, sieving the used powder, storage, and documentation. Empirical factors for extra effort under inert environment have been removed from the original model.

$$C_{Removal}(P_i) = (C_{op} + C_{mach}) \cdot \frac{T_{Rem}}{\sum_i N_i} \qquad (9)$$

where:
$C_{Removal}$ is the cost per part for removing the substrate/parts from the AM machine ($),
P_i is the built-up AM part corresponding to ith geometry (-),
T_{Rem} is the time required to remove parts, clean machine, and perform all ancillary tasks (h),
C_{oper} is the operator's hourly rate ($/hour),
C_{Mach} is the AM machine's hourly operating cost ($/h),
N_i is the quantity of parts with ith geometry (-).

The next step involves separation of parts from the build substrate. Modifying the original formula [16], parts produced in a build job using laser-powered PBF may have built-up residual stress and thus undergo a stress-relief [49] to reduce geometric distortion upon separation. Once completed, wire electrical discharge machining (EDM) is used to physically

detach all parts from the substrate. The costs for wire EDM are allocated based on the contact area occupied by a part, and their support structures, on the substrate as follows in Equation 10.

$$C_{Substrate}(P_i) = \frac{C_{stress}}{\sum_i N_i} + C_{EDM} \cdot \frac{A_{con}(G_i)}{\sum_i N_i \cdot A_{con}(G_i)} \qquad (10)$$

where:
$C_{Substrate}$ is the cost per part for separating a part from the substrate ($),
P_i is the built-up AM part corresponding to ith geometry (-),
C_{stress} is the cost for stress-relieving a build plate($),
C_{EDM} is the total cost for separating a part via EDM ($),
A_{con} is the connected area of a part to the substrate (cm^2),
N_i is the quantity of parts with ith geometry (-).

Once all parts have been separated from the build substrate, these components can undergo additional post-processing to meet customer requirements. Due to parts having individually-tailored functions and applications, the required operations and sequence of their events will vary due to the specifications ordered by the costumer. For Equation 11 [16], cost is calculated for post-processing based on support structure removal for an individual part. The time for post-processing is a function of the part's geometric complexity and can increase if additional time or equipment is needed. For estimation purposes, the equation is broad and can be extended to encompass additional post-processing operations as designated by the user.

$$C_{postp}(P_i) = \sum_i \left(T_{postp}(G_i) \cdot (C_{op} + C_{tools}) \right) \qquad (11)$$

where:
C_{postp} is the total cost for post-processing ($),
P_i is the built-up AM part corresponding to ith geometry (-),
T_{postp} is the time required to post-process a part geometry ($),
G_i is the ith geometry (-),
C_{op} is the operator's hourly rate ($/hour),
C_{tools} is the hourly rate of tools and machines for post-processing ($).

In summary, this cost model consists of 7 activities in the AM workflow (see Figure 7). Costs are allocated based on an AM operator's labor for part preparation, arranging geometries on the build tray, setting-up the AM machine, executing the build job, and removing the substrate and decommissioning the machine. Afterwards, post-processing of the build job begins with stress-relief, wire EDM, followed last by individual post-processing to produce a fully-functional component. These 7 activities are added together in Equation 12 to produce the total cost for a part made using PBF:

$$C_{Total}(P_i) = C_{prep}(P_i) + C_{buildjob}(P_i) + C_{Setup}(P_i) + C_{Build}(P_i) + C_{Removal}(P_i)$$

$$+ C_{Substrate}(P_i) + C_{Postp}(P_i) \qquad (12)$$

where:

C_{total} is the total manufacturing costs (\$),

C_{prep} is the cost per part for preparing the digital geometry data (\$),

$C_{buildjob}$ is the cost per part for the build tray assembly (\$),

C_{setup} is the cost for setting up the machine (\$),

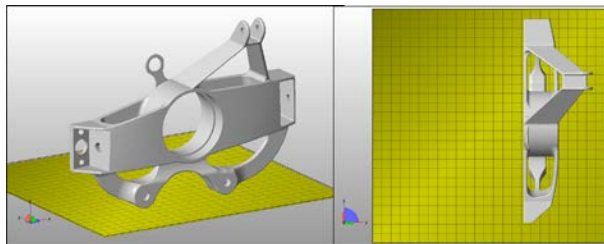C_{build} is the cost for building up a part in the AM process (\$),

$C_{Removal}$ is the cost for removing the substrate/parts from the machine (\$),

$C_{Substrate}$ is the cost for separating a part from the substrate (\$),

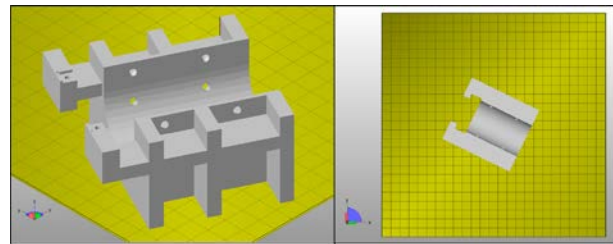C_{postp} is the total cost for post-processing (\$).

4. Implementation and Case Study

To demonstrate this approach, costs were studied for two parts designed for and produced by laser-based PBF. Figures 8 and 9 show the geometric data and build orientation for each of the parts, which were built using EOS Titanium Ti64 and Stainless Steel GP1, respectively. These parts were selected because Ti64 is a high-value material and GP1 is relatively cheaper. All parts were manufactured on an EOSINT M280 DMLS machine at Penn State's Center for Innovative Materials Processing through Direct Digital Deposition (CIMP-3D). Following the workflow of Rickenbacher et al., STL files were first imported into Materialise Magics for digital preparation and support structure generation. Geometries were then entered into EOS RP Tools and sliced to form the build job file. Next, the files were entered into EOS PSW, where process parameters were selected, and then the AM process commenced. Once completed, the build substrate was removed from the machine, the machine was cleaned, powder was sieved, and build documentation was completed. Finally, the parts and substrate were shipped to a local manufacturer for stress-relief and wire EDM, before returning to CIMP-3D for post-processing.

Geometry	G_1
N_i	1
V_{part} (cm³)	175
$V_{supports}$ (cm³)	412
V_{total}(cm³)	587
A_{con}(cm²)	69
Bounding Box (mm)	74 x 218 x 172

Figure 8: Automotive Upright – Geometry G_1

Geometry	G_2
N_i	1
V_{part} (cm³)	95
$V_{supports}$ (cm³)	97
V_{total}(cm³)	192
A_{con}(cm²)	59
Bounding Box (mm)	76 x 84 x 47

Figure 9: Testing Apparatus– Geometry G_2

All equations from Section 3 were written in a MATLAB program and used for costing each of the builds. For this case study, constants for powder losses due to process inefficiency (α) and powder trapped in support structures (γ) were chosen to be 40% and 25%, respectively, based on CIMP-3D staff's experience from three years of producing metal AM parts at the facility [48]. Unique to laser-powered PBF is that the part bed lowers by a layer thickness and

the feed bed dispenser platform rises between "2x or 2.5x" [7] the layer thickness to account for changes in powder levelling during thermal consolidation. The ratio of the vertical rise of the feed bed to the lowering of the part bed shall be referred to as CA, also known as charge [50]. If CA is set too low by the user, then the build can be prone to powder shorting and insufficient coverage of the build plate [7, 50]. Thus, with the guidance of the CIMP-3D staff, a CA of 2.25 was assumed to be sufficient for all build jobs in this case study. Equation 13 was used to estimate the mass of powder loaded in the feed bed for a generic laser-powered PBF machine. A list of constants used in the cost model for these two examples are included in Table 1.

$$M_{FB} = CA \cdot D_x \cdot D_y \cdot Bh(P_i) \cdot \rho_t \tag{13}$$

where:
M_{FB} is the total mass of the powder loaded into the AM machine's feed bed (kg),
CA is the vertical rise of the feed bed per layer thickness in the build (-),
D_x is the length of the dispenser platform in the feed bed (mm),
D_y is the width of the dispenser platform in the feed bed (mm),
Bh is the build height of the tallest part in the build job (mm),
ρ_t is the powder tap density (kg/cm^3).

Table 2 contains all the values used in the cost model for the two example parts. These values were collected from material datasheets available from the manufacturer [51, 52]. Since the feedstocks have a wide range of permissible reuses, costs were modeled parametrically by varying the maximum allowable build cycles, U_{max}, between 10, 20, 30, and 40, to correspond with the data found in the literature review. The graph in Figure 10 shows an example of the cost for a powder feedstock at each of the maximum build cycles. Each point represents the financial value of a powder feedstock with the given number of accumulated reuses. The salvage value, estimated resale value, of a powder that exceeded the maximum amount of build cycles was assumed to be zero.
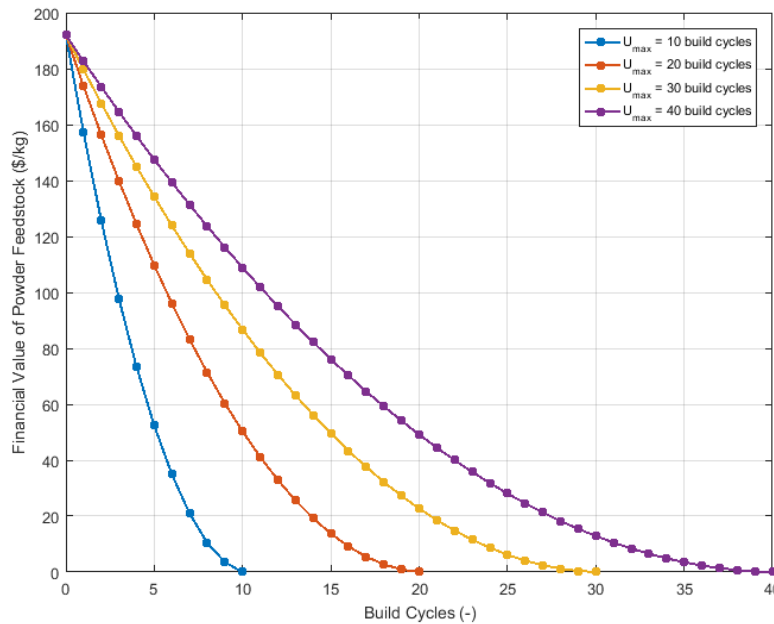

Figure 10: Powder Feedstock Value vs. Build Cycles vs. Maximum Build Cycles

Table 1: Cost Model Constants

Variable	Description	Value	Units
C_{oper}	Operator's hourly rate	110	$/h
C_{pc}	Cost for using computer workstation with all software and licenses	100	$/h
C_{Mach}	AM machine's hourly rate	60	$/h
C_{gas}	Cost for inert gas consumption during the build	10	$/h
$T_{buildjob}$	Time required for arranging all geometries in the build job	1	h
T_{setup}	Time required to set up the AM machine	2	h
$T_{mat.change}$	Time for changing and loading new powder into AM machine	3	h
T_{idle}	Time when AM machine is inactive in build (startup, heating, cooling)	-	h
$T_{recoat\,rate}$	Average time for AM machine to spread one layer of powder	9	sec
T_{rem}	Time required to remove substrate and clean machine after build	3	h
α	Percentage of powder loss due to process inefficiency	40	%
γ	Percentage of powder loss due to entrapment in support structures	25	%
T_{Rem}	Time required to remove parts, clean machine after build	3	h
C_{stress}	Total cost for thermally processing all parts on build substrate	350	$
C_{EDM}	Total cost for separating all parts on substrate via EDM	200	$
C_{tools}	Cost for work area with tools and machines for post-processing	50	$
CA	Vertical rise of the feed bed per layer thickness in the build	2.25	-
D_x	Length of the dispenser platform in the feed bed	228	cm
D_y	Width of the dispenser platform in the feed bed	250	cm
Sb_x	Length of the build substrate platform in the part bed	250	cm
Sb_y	Width of the build substrate platform in the part bed	250	cm

Table 2: Material Constants

Material	ρ_t (g/cm^3)	ρ_w (g/cm^3)	L_T (μm)	$T_{build\,speed}$ (h/cm^3)	Cm_0 $($/kg)$	S $($)$	U_{max} $(-)$
Ti64	2.74	4.41	30	13.5	680	-	{10,20,30,40}
GP1	5.3	7.8	20	7.2	100	-	{10,20,30,40}

5. Results and Discussion

5.1. Labor Time and Build Results

Table 3 lists build data for the two example parts. Geometry G_1 had a build time of 55 hours, and Geometry G_2 had a build time of 31 hours. The estimated build time was over-predicted for both parts by 6%. This discrepancy is attributed to the assumption that T_{idle} is zero for preheating, machine cool-down, and laser positioning between hatches during the build process. G_1 required 61 kg of powder to perform the build, whereas G_2 required 32 kg. At the time of this study, there was insufficient records that documented the build cycles endured by the powder feedstocks used in the production of the two example parts. To accommodate for this lack of information, costing scenarios were generated for all material reuses ranging from virgin powder, reused powder, and powders that reached their maximum allowable build cycles.

Table 3: Labor Time and Build Results

Part	Material	N_i (−)	V_{total} (cm³)	Bh (mm)	T_{prep} (h)	T_{build} estimate (h)	T_{build} actual (h)	T_{postp} (h)	M_i (kg)	M_{FB} (kg)
G_1	Ti64	1	587	172	3	58	55	3	3.9	61
G_2	GP1	1	192	47	2	33	31	2	2.2	32

5.2. Costing for Example Parts

Figure 11 shows the range of total costs, including all labor activities, for Geometry G_1 as a function of the build cycles endured by the feedstock loaded for the build job. The points along the graph represent the cost for a build job loaded with a powder feedstock with the given number of reuses. Powders having a U_{max} of 10 build cycles were the most expensive due to having the shortest allowable reuses and therefore the most rapid decline in value. Meanwhile, powders with a 40 build cycle limit had a longer reuse duration and thus a slower rate of decline.

The total cost for manufacturing these parts ranged among virgin powders, represented as zero build cycle feedstocks, between $11,000 and $16,500. The lowest cost scenario was the use of a powder that exceeded the maximum amount of permissible build cycles (i.e., powder that is chemically out-of-specification, diminished flowability, etc.), and total costs were $6800. This is because as a powder is increasingly reused, $C_{build-material}$ and $C_{build-depreciation}$ decrease in proportion to the diminishing financial value of the powder feedstock with each build cycle. At this lower limit, the feedstock's value has been reduced to the salvage value, zero for this case study. Hence, the material cost has diminished and the depreciation cost has become zero, due to a zero difference in the financial value of a feedstock that has become a scrap material.
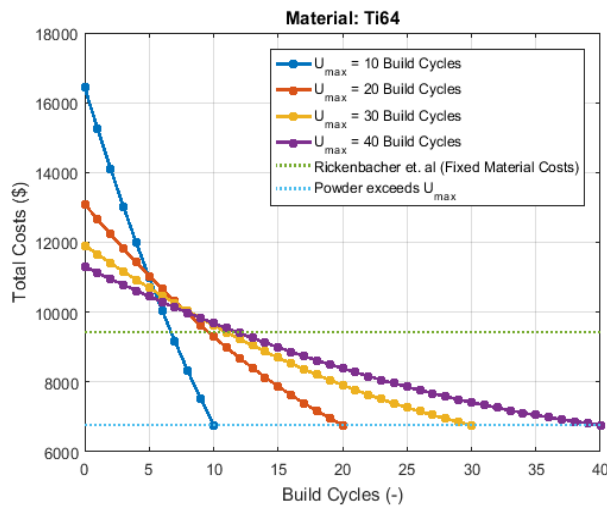

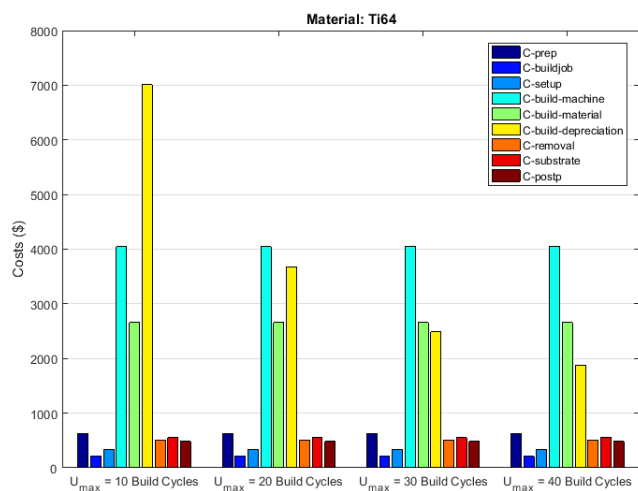Figure 11: Total Costs vs. Build Cycles for Powder Reuse for Geometry G_1

Figure 12: Cost for Workflow Activities for Geometry G_1 with Virgin Powder

The previous Rickenbacher et al. model, which used fixed material costs, had a constant value of $9400, regardless of the reuses accumulated by the input powder. In comparison to the cost scenarios accounting for reused powders, *the fixed material cost method undervalued the cost of build jobs with virgin Ti64 powder within a range of 13% and 75%.* After 7 and/or 13 build cycles, the fixed material cost model started to overvalue total costs and thus, build jobs

using a powder that had surpassed these cycles could achieve a cost savings. The largest cost savings was a 38% reduction compared to the fixed material cost method, specifically when using a powder that exceeds its useful life (U_{max}).

Figure 12 shows a cost breakdown using virgin powder and each of their maximum reuses. The top three costs are $C_{build-depreciation}$, $C_{build-machine}$, and $C_{build-material}$. The depreciation cost was the largest cost for a powder with a 10 build cycle limit at 42% of the total cost. When U_{max} was greater than 20 build cycles, the depreciation cost was overtaken by the machine cost, and subsequently minimized to 17% of costs when U_{max} was equal to 40 build cycles. In comparison, the depreciation costs were more than 2.6 times the material costs.

Similar analysis was conducted on Geometry G_2 and displayed in Figures 13 and 14. Builds using virgin GP1 powder had a range between $5000 and $5500. The lower limit for builds using powders that exceeded U_{max} was $4600. Using the fixed material cost model as the reference, which valued the builds at approximately $4900, *virgin GP1 powder builds were undervalued between 3% and 11%, depending on the maximum reuses permitted for the feedstock.* Upon surpassing 6 and/or 11 build cycles, the totals costs became overvalued, and thus a cost savings of 5% could be achieved by building with a powder outside the allowable for U_{max}. The largest cost for Geometry G_2 was $C_{build-machine}$ at 42%, $C_{build-depreciation}$ at 11%, and C_{postp} at 10% of the total costs. Similar to Geometry G_1, when using a 10 build cycle maximum virgin powder, the depreciation cost was twice that of the material costs.
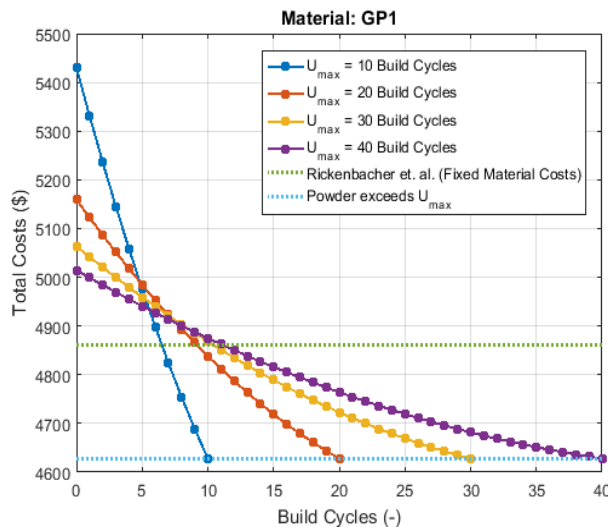

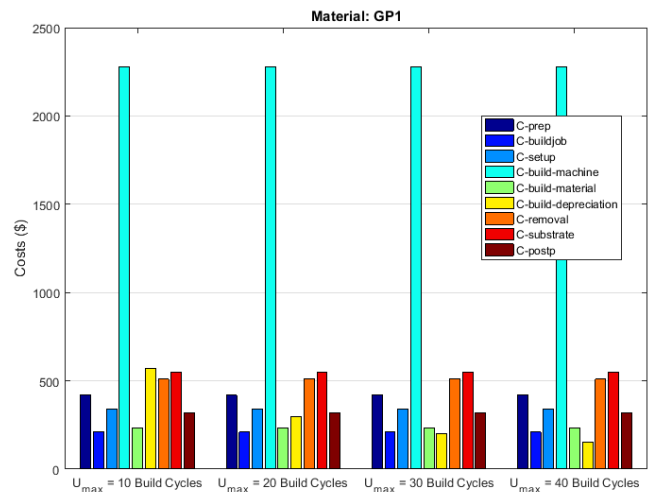Figure 13: Total Costs vs. Build Cycles for Powder Reuse for Geometry G_2

Figure 14: Cost for Workflow Activities for Geometry G_2 with Virgin Powder

5.3. Summary of Results

The costing for these two example parts revealed that the machine cost, $C_{build-machine}$, was the most pervasive cost for both builds. This is due to the volume of the geometries and support structures being consolidated during processing, their corresponding build heights, and the build speeds at which the DMLS machine can melt the given material. The labor activities pertaining to $C_{buildjob}$, C_{setup}, $C_{removal}$, and $C_{substrate}$ showed no significant cost fluctuation

among the example parts. This is because these activities are standardized procedures with average completion times based on the skill of the AM operator and independent of the geometries in the build. While C_{prep} and C_{postp} can vary for complex geometries requiring support structures, these costs ranged between 3-11% of the costs in all of the builds, due to larger costs being attributed to machine time, material, and deprecation.

Depreciation was one of the largest costs for Geometries G_1 and G_2. It was at most 42% of the total costs for G_1 but only 11% in G_2. When looking specifically at G_1 and its use of Ti64 powder, the relatively larger depreciation cost in comparison to G_2 is due to G_1 requiring nearly twice as much powder to fill the feed bed due to differences in tap densities and part build heights, along with the Ti64 powder being nearly seven times more expensive than GP1. The machine cost had a relatively higher percentage in GP1 because of its 20 micron layer thickness and 7.2 h/cm^3 build speed, which was half the speed when using Ti64. In both examples, when using a powder with a U_{max} of 10 build cycles, the depreciation cost was greater than twice the cost of the melted material. One interpretation for this result is that the utilized build envelope (i.e., volume packing) [53] is uneconomical for the given build since the surrounding un-melted powder is being put at risk of contamination and degradation, and thus more costly than the built-up parts produced in the AM process. Given that the depreciation cost is calculated as the difference between the mass of the un-melted powder and the mass of powder melted for the parts, a highly packed build tray with a high quantity and large mass of produced parts could reduce the overall depreciation costs since more of the surrounding powder would be melted and consumed during the build job. Less un-melted powder would remain after the build and thus, the costs for the material could be more economical than the depreciation, however post-processing costs may increase as a result of the additional part quantities.

5.4. Model Limitations

Uncertainties in the model are the exact number of reuses permitted for each material alloy, an open and active area of research in the metal AM community. The parametric analysis accounted for 4 different maximum build cycle limits, but literature and standards are limited that provide recommendations on the exact extent for which a reused metal powder can be used to produce AM parts in functional engineering applications (e.g., aerospace, biomedical, etc.). This model did not consider the use of alternative powder feedstocks not officially offered by the OEM, which may have lowered costs and altered process parameters. However, the use of unauthorized materials run the risk of voiding AM machine warranty agreements. Since the powder is selectively melted with each build job, the remaining un-melted powder lot would require additional powder to be added in order to reproduce the same build job. Thus, a cost would have to be allocated for adding virgin powder to a reused powder lot in production. Post-processing accounted for the removal of support structures; however, functional components may call for more sophisticated processes such as annealing, shot peening, or CT (computed tomography) scanning in order to validate the integrity of the part. While these examples considered DMLS, costing for EBM will have differences due to variations in PBF technology and required labor activities. In addition, the empirical waste factors in calculating the part mass were specific to an EOSINT M280 and may not be applicable to other PBF processes. Finally, costs for the re-design and engineering of a pre-existing component in order to be made using AM were not captured in this model.

6. Closing Remarks

A cost model was created for reused metal powder feedstocks using SOYD depreciation to account for costs pertaining to the diminishing and depletion of a metal powder feedstock's properties in PBF. This depreciation model was implemented in a generic activity-based costing model for PBF. A case study was presented using Ti64 and GP1 parts produced using DMLS. Costs for individual parts showed that $C_{build-machine}$ and $C_{build-depreciation}$ were the top two costs, whereas labor activities were relatively stagnate and less costly. With reference to cost models with fixed material costs, the depreciation costs due to lost value from reusing a metal powder feedstock added an additional 13-75% in cost for build jobs with virgin powders using Ti64, or 3-11% for GP1. Upon exceeding 13 build cycles in Ti64, 11 for GP1, the total costs for build jobs achieved a cost savings of 38% or 5% when using a highly reused powder or powder feedstock exceeding its useful life (U_{max}). The practicality of using a highly reused powder feedstock will vary based on material type, PBF technology, and the functional application of the resulting component.

Future improvements to this model could explore more detailed costing options for post-processing. The financial implications of volume packing and adding virgin powder to a reused powder lot could be explored to better understand building scenarios that are most applicable to high volume production in industry. Although this study considered the cost for two individually produced components, the supply chain and economics of mass production could be modeled to study the impact of accounting for reused powders. One improvement would be the creation of a standardized metric for measuring the overall quality and reusability of the powder feedstock in a PBF technology to aid in formalizing the financial value and acceptability for a reused powder. Finally, further material science research on metal powder feedstocks for AM can help broaden the literature that quantifies mechanical properties and the engineering limitations of these materials as they are continually adopted in full-functional components.

Acknowledgments

References

[1] ASTM F2792 - 12a Standard Terminology for Additive Manufacturing Technologies. *ASTM International*, https://www.astm.org/Standards/F2792.htm, Accessed: 14 Oct. 2015.
[2] Gibson, I., D. W. Rosen, and B. Stucker, 2010. Additive manufacturing technologies: rapid prototyping to direct digital manufacturing. Springer, New York.
[3] Frazier, W.E., 2014. "Metal additive manufacturing: a review." *Journal of Materials Engineering and Performance*, *23*(6), pp.1917-1928.
[4] Hussein, A., Hao, L., Yan, C., Everson, R. and Young, P., 2013. "Advanced lattice support structures for metal additive manufacturing." *Journal of Materials Processing Technology*, *213*(7), pp.1019-1026.

[5] Sochalski-Kolbus, L.M., Payzant, E.A., Cornwell, P.A., Watkins, T.R., Babu, S.S., Dehoff, R.R., Lorenz, M., Ovchinnikova, O. and Duty, C., 2015. "Comparison of residual stresses in Inconel 718 simple parts made by electron beam melting and direct laser metal sintering." *Metallurgical and Materials Transactions A*, *46*(3), pp.1419-1432.

[6] Béraud, N., Vignat, F., Villeneuve, F. and Dendievel, R., 2014. "New trajectories in Electron Beam Melting manufacturing to reduce curling effect." *Procedia CIRP*, *17*, pp.738-743.

[7] Moylan, S.P., Slotwinski, J.A., Cooke, A.C., Jurrens, K. and Donmez, M.A., 2013. "Lessons Learned in Establishing the NIST Metal Additive Manufacturing Laboratory." *NIST Technical Note 1801*, http://nvlpubs.nist.gov/nistpubs/TechnicalNotes/NIST.TN.1801.pdf

[8] Bhavar, V., Kattire, P., Patil, V., Khot, S., Gujar, K. and Singh, R., 2015. "A Review on Powder Bed Fusion Technology of Metal Additive Manufacturing." In *International Conference & Exhibition on Additive Manufacturing Technologies,* Bangalore, India.

[9] Medina, F., 2013. "Reducing metal alloy powder costs for use in powder bed fusion additive manufacturing: Improving the economics for production." *Ph.D. Dissertation*, University of Texas, El Paso, http://digitalcommons.utep.edu/dissertations/AAI3611283

[10] Dawes, J., Bowerman, R. and Trepleton, R., 2015. "Introduction to the additive manufacturing powder metallurgy supply chain." *Johnson Matthey Technology Review*, *59*(3), pp.243-256.

[11] Slotwinski, J.A., Garboczi, E.J., Stutzman, P.E., Ferraris, C.F., Watson, S.S. and Peltz, M.A., 2014. "Characterization of metal powders used for additive manufacturing." *Journal of Research of the National Institute of Standards and Technology*, *119*, pp. 460-493.

[12] Slotwinski, J.A. and Garboczi, E.J., 2015. "Metrology needs for metal additive manufacturing powders." *JOM*, *67*(3), pp.538-543.

[13] Slotwinski, J.A., Garboczi, E.J. and Hebenstreit, K.M., 2014. "Porosity measurements and analysis for metal additive manufacturing process control." *Journal of Research of the National Institute of Standards and Technology*, *119*, pp. 494-528.

[14] "Measurement Science Roadmap for Metal-Based Additive Manufacturing." *National Institute of Standards and Technology*. May 2013. Web. 15 Oct. 2015. <http://www.nist.gov/el/isd/upload/NISTAdd_Mfg_Report_FINAL-2.pdf>.

[15] Lindemann, C., Jahnke, U., Moi, M. and Koch, R., 2012, August. "Analyzing product lifecycle costs for a better understanding of cost drivers in additive manufacturing." In *23rd Annual International Solid Freeform Fabrication Symposium–An Additive Manufacturing Conference*. Austin, TX 6th-8th August.

[16] Rickenbacher, L., Spierings, A. and Wegener, K., 2013. "An integrated cost-model for selective laser melting (SLM)." *Rapid Prototyping Journal*, *19*(3), pp.208-214.

[17] ASTM B243 - 13 Standard Terminology for Powder Metallurgy. *ASTM International*, 7 Jan. 2015.

[18] Maringer, R. and Patel, A., "Patent WO1989000471A1 - Centrifugal Disintegration." *World Intellectual Property Organization*, 26 Jan. 1989. Web. 4 Jan. 2016.

[19] Howells, R., Stoner, G. and Stockumas, J., "Patent: US4880162 - Gas Atomization Nozzle for Metal Powder Production." *USPTO Patent Database*. 14 Nov. 1989.

[20] Sidney, I., Clark, R., and Baltrukovicz, B., "Patent US4080126 - Water Atomizer for Low Oxygen Metal Powders." *USPTO Patent Database*. 21 Mar. 1978.

[21] Axelsson, S., 2012. "Surface Characterization of Titanium Powders with X-ray Photoelectron Spectroscopy." Doctoral dissertation, Chalmers University of Technology, Gothenburg, Sweden.

[22] Silberberg, M.S., Duran, R., Haas, C.G. and Norman, A.D., 2006. *Chemistry: The molecular nature of matter and change* (Vol. 4). New York: McGraw-Hill.

[23] Watkins, K.G., Steen, W. and Mazumder, J., 2010. "Laser Material Processing." Springer.

[24] Jamshidinia, M., Sadek, A., Wang, W. and Kelly, S., 2015. "Additive manufacturing of steel alloys using laser powder-bed fusion." Advanced Materials & Processes, *173*(1), pp.20-24.

[25] ASTM F2924 – 14 Standard Specification for Additive Manufacturing Titanium-6 Aluminum-4 Vanadium with Powder Bed Fusion." *ASTM International*, Web. 7 Jan. 2015.

[26] ASTM F3001 – 14 Standard Specification for Additive Manufacturing Titanium-6 Aluminum-4 Vanadium ELI with Powder Bed Fusion." *ASTM International*, Web. Accessed: 7 Jan. 2015.

[27] ASTM F3055-14a Standard Specification for Additive Manufacturing Nickel Alloy (UNS N07718) with Powder Bed Fusion." *ASTM International*, Web. Accessed: 7 Jan. 2015.

[28] ASTM F3056 – 14e1 Standard Specification for Additive Manufacturing Nickel Alloy (UNS N06625) with Powder Bed Fusion." *ASTM International*, Web. Accessed: 7 Jan. 2015.

[29] Seyda, V., Kaufmann, N. and Emmelmann, C., 2012. "Investigation of aging processes of Ti-6Al-4 V powder material in laser melting." *Physics Procedia*, *39*, pp.425-431.

[30] Tang, H.P., Qian, M., Liu, N., Zhang, X.Z., Yang, G.Y. and Wang, J., 2015. "Effect of powder reuse times on additive manufacturing of Ti-6Al-4V by selective electron beam melting." *JOM*, *67*(3), pp.555-563.

[31] Grainger, L. "Investigating the effects of multiple re-use of Ti6Al4V powder in additive manufacturing (AM)," *Renishaw plc*, UK. Web. Accessed: 26 June 2016. <http://www.renishaw.com/en/blog-post-how-much-can-you-recycle-metal-additive-manufacturing-powder--38882>

[32] Ardila, L.C., Garciandia, F., González-Díaz, J.B., Álvarez, P., Echeverria, A., Petite, M.M., Deffley, R. and Ochoa, J., 2014. "Effect of IN718 recycled powder reuse on properties of parts manufactured by means of selective laser melting." *Physics Procedia*, *56*, pp.99-107.

[33] Gale Encyclopedia of American Law. 2010. Depreciation. Donna Batten, Ed. 3rd ed. Vol. 3. Detroit, MI: Gale. 427-428. *Gale Virtual Reference Library*. Accessed: 17 Oct. 2015.

[34] Internal Revenue System, "Overview of Depreciation," *U.S. Department of Treasury*, Web. Accessed: 17 Oct. 2015. <https://www.irs.gov/publications/p946/ch01.html#en_US_2013_ publink1000107337>

[35] Newnan, D.G., Eschenbach, T. and Lavelle, J.P., 2004. *Engineering economic analysis.* Vol. 2. Oxford University Press, Oxford, UK.

[36] Samperi, M., "Development of Design Guidelines for Metal Additive Manufacturing and Process Selection." *M.S. Thesis*, Mechanical Engineering, The Pennsylvania State University. June 2014.

[37] EOS GmbH, Basic Design Rules for Additive Manufacturing, Electro Optical Systems, Germany. Web. Accessed: 15 Oct. 2015.

[38] Kannan, T., "Design for Additive Manufacturing." *Geometric Global*. Web. Accessed: 15 Oct. 2015.

[39] "netfabb Support Structures." *netfabb Gmbh.* <http://www.netfabb.com/support_structures.php>. Web. Accessed: 3 Jan. 2016

[40] "Magics SG+ Module" *Materialise NV.* <http://software.materialise.com/magics-sg-plus-module>. Web. Accessed: 3 Jan. 2016

[41] Wright, S. 2015, "A Story of Failure and Success in Metal AM: The Reality of Developing a Titanium Bike Part." *Metal Additive Manufacturing Magazine*. Vol .1, No.3.

[42] Vayre, B., Vignat, F. and Villeneuve, F., 2013. "Identification on some design key parameters for additive manufacturing: application on electron beam melting." *Procedia CIRP*, *7*, pp.264-269.

[43] Office of Environmental Health and Safety, *Waste Management Log Book*, The Pennsylvania State University. < http://abe.psu.edu/safety/lab-safety-plan/chemical-waste/chemical-waste-log-book> Accessed: 30. Aug. 2016.

[44] Oller, A.R., Kirkpatrick, D.T., Radovsky, A. and Bates, H.K., 2008. "Inhalation carcinogenicity study with nickel metal powder in Wistar rats." *Toxicology and applied pharmacology*, *233*(2), pp.262-275.

[45] Jacobson, M., Cooper, A.R. and Nagy, J., 1964. "Explosibility of metal powders." U.S. Bureau of Mines, Washington, D.C.

[46] Wright, Spencer. "Notes on Magics." 18 Aug. 2015. Web. Accessed: 15 Jan. 2016. <http://pencerw.com/feed/2015/8/18/notes-on-magics>.

[47] Baumers, M., C. Tuck, R. Wildman, I. Ashcroft, E. Rosamond, and R. Hague. "Combined Build-Time, Energy Consumption and Cost Estimation for Direct Metal Laser Sintering." In *From Proceedings of Twenty Third Annual International Solid Freeform Fabrication Symposium—An Additive Manufacturing Conference*, vol. 13. 2012, Austin, TX.

[48] Zelinski, P., 2015. "Additive's Idiosyncrasies." *Additive Manufacturing*, February, 4-9.

[49] Thöne, M., Leuders, S., Riemer, A., Tröster, T. and Richard, H.A., 2012. "Influence of heat-treatment on selective laser melting products–eg Ti6Al4V." *International Solid freeform fabrication symposium,* Austin, TX.

[50] Foster, B.K., Reutzel, E.W., Nassar, A.R., Hall, B.T., Brown, S.W. and Dickman, C.J., "Optical, layerwise monitoring of powder bed fusion." *International Solid Freeform Fabrication Symposium Proceedings* (pp. 295-307).

[51] EOS GmbH – Electro Optical Systems, "EOS Stainless Steel GP1", Material Data Sheet, Germany. Web. Accessed: 15 Oct. 2015.

[52] EOS GmbH – Electro Optical Systems, "EOS Titanium Ti64", Material Data Sheet, EOS GmbH – Electro Optical Systems, Germany. Web. Accessed: 15 Oct. 2015.

[53] Baumers, M., Tuck, C., Wildman, R., Ashcroft, I. and Hague, R., 2011. "Energy inputs to additive manufacturing: does capacity utilization matter?" *EOS*, *1000*(270), pp. 30-40.